

## P2.56 ASSESSING TROPICAL CYCLONE FLOOD RISK IN AUSTRALIA – IMPLICATIONS FOR CATASTROPHE MODELING

Jason T. Butke\*, Peter Sousounis, and Kevin Hill  
AIR Worldwide Corporation, Boston, Massachusetts

### 1. INTRODUCTION

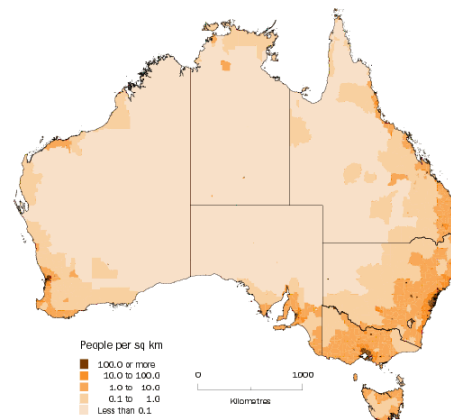
Annually, approximately 16 tropical cyclones develop in the Southwest Pacific and Southeast Indian Ocean basins (Fig. 1). Half of those intensify into severe tropical cyclones (wind speeds > 117 km/hr) while about 4 or 5 make landfall in Australia.

In the last half century, precipitation induced flooding from landfalling tropical cyclones has likely become the largest threat to human life. The economic impact can also be significant. In 1974, for example, flooding from cyclone Wanda caused the worst tropical cyclone induced flooding in the 20<sup>th</sup> century in Queensland, resulting in as much as \$200 AUD million economic loss (1974 dollars; \$7000 AUD million, in 2010 dollars).

Historically, in Australia, wind damage dominates tropical cyclone losses; however, freshwater flooding has also caused significant property loss.

A modeling case study is conducted for the Brisbane River watershed (Fig. 3) for cyclone Wanda (1974), whereby precipitation output from the WRF model is used as input to a 2-dimensional rainfall-runoff model, based on the CASCade 2 Dimensional (CASC2D).

Australia has the 11<sup>th</sup> largest non-life insurance market in the world and like the United States, the majority of population is along the coast (Fig. 2), with several cities (e.g. Darwin, Cairns, Brisbane) located in tropical cyclone prone regions (Fig. 1). Cyclone damage (wind and flooding) is almost always included with homeowner and commercial policies under windstorm coverage.



Source: ABS, 2009, [Regional Population Growth, Australia 2007-08](#) (cat. no. 3218.0).

Figure 2. Australia Population Density

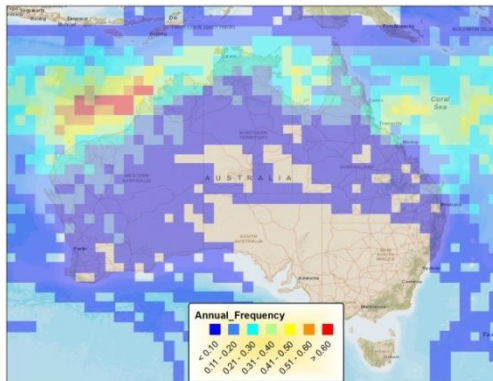


Figure 1. Historical Frequency (1951-2009; Bureau of Meteorology)

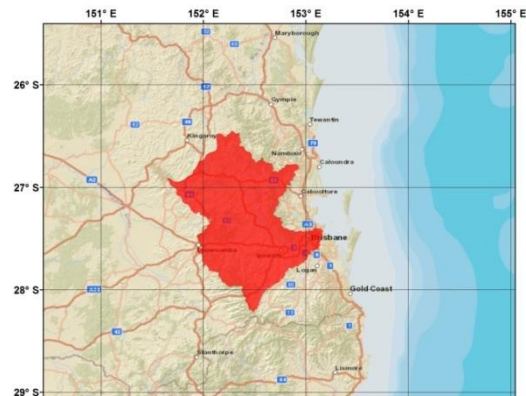


Figure 3. Brisbane River Watershed

\* Corresponding author address: Jason T. Butke,  
AIR Worldwide Corporation, Boston, MA 01960;  
e-mail: [jbutke@air-worldwide.com](mailto:jbutke@air-worldwide.com).



resolve the mesoscale features associated with cyclone Wanda. NCEP/NCAR Reanalysis Project (NNRP R1; pgb.f00 and grb2d) 2.5° data was used for initial and lateral boundary conditions. Analysis nudging of the outer domain was tested with only marginal differences to running without.

Table 1 summarizes the physics options used. Various sensitivity tests of different parameterization schemes, horizontal resolution, and initialization time (Wanda portion only) were conducted. Because precipitation was the primary focus of this study, emphasis was placed on microphysics and cumulus schemes. WRF Single-Moment 6-class (WSM-6) microphysics and Betts-Miller-Janjic (BMJ) cumulus schemes were ultimately chosen for all simulations except during the Wanda phase (January 23-29) where no explicit convection was utilized for the innermost domain due to the high grid resolution. That combination provided the best match to observations. Hourly precipitation was used as input to CASC2D.

Physics Options	Schemes
Microphysics	WSM-6
Longwave Radiation	RRTMG
Shortwave Radiation	Dudhia
Surface Layer	MM5 Similarity
Land Surface	5-layer thermal diffusion
PBL Layer	Yonsei University
Cumulus	Betts-Miller-Janjic
Cumulus <sup>1</sup>	No Cumulus

Table 1. Physics parameterizations used in all WRF runs. <sup>1</sup>January 23 through January 29.

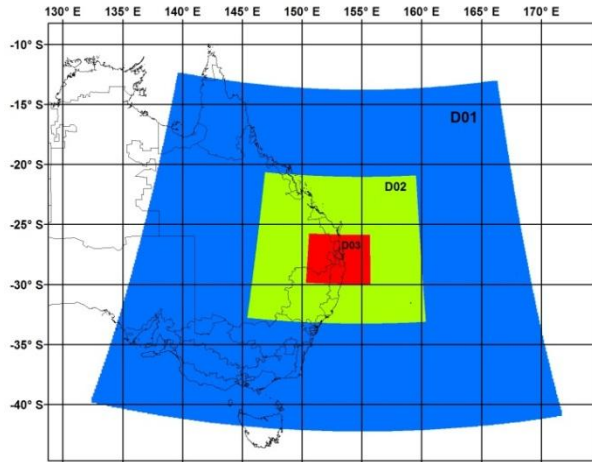


Figure 6. WRF model computational domains

### 3.2 CASC2D

Precipitation-induced flooding is modeled dynamically, based on the two-dimensional rainfall runoff CASC2D-SED (CASCade 2 Dimensional SEDiment) model developed at Colorado State University (Rojas *et al.*, 2003).

The shallow water equations (also called the Saint Venant equations) are the basis of the model, which are derived from the equations of conservation of mass, energy, and momentum (so-called primitive equations). The shallow water equations are appropriately used in models where the horizontal length scale is much greater than the vertical, as is the case with this model, where the horizontal resolution is 180 meters.

$$\text{mass continuity: } e = \frac{\partial h}{\partial t} + \frac{\partial q_x}{\partial x} + \frac{\partial q_y}{\partial y}$$

$$x - \text{momentum: } g \left( S_{ox} - S_{fx} - \frac{\partial h}{\partial x} \right) = \frac{\partial u}{\partial t} + u \frac{\partial u}{\partial x} + v \frac{\partial u}{\partial y}$$

$$y - \text{momentum: } g \left( S_{oy} - S_{fy} - \frac{\partial h}{\partial y} \right) = \frac{\partial v}{\partial t} + u \frac{\partial v}{\partial x} + v \frac{\partial v}{\partial y}$$

where  $e$  is precipitation excess (precipitation – infiltration – evaporation; mm),  $h$  is surface depth (m),  $t$  is time (s),  $q_x$  and  $q_y$  are flow rates in the  $x$  and  $y$  directions (m/s),  $x$  and  $y$  are cell sizes (m),  $g$  is the gravitation acceleration ( $9.8 \text{ m s}^{-2}$ ),  $S_{o(x,y)}$  are bed

slopes in the  $x$  and  $y$  directions,  $S_{f(x,y)}$  are friction slopes in the  $x$  and  $y$  directions, and  $u$  and  $v$  are average velocities in the  $x$  and  $y$  directions (m/s)

To handle complex terrain, CASC2D was modified to account for eight possible directions of movement, rather than two.

CASC2D was also modified to explicitly account for evaporation and vegetation interception (assumed constant, at  $1 \text{ mm hr}^{-1}$ ), based on mean daily pan evaporation rates in the summer months in Australia and average vegetation interception rates for mature forests. Various code efficiencies were also implemented.

Data requirements are hourly precipitation, elevation, vegetation, soil, a land/sea mask, and outlet cells (grid cells which empty into the ocean). Figure 7 details the SRTM 90-m elevation data (Farr *et al.*, 2007).

The model explicitly accounts for spatially varying rainfall, infiltration, evaporation/vegetation interception, overland flow, and flow routing (Fig. 8). Due to the grid

resolution, channel flow was not considered and sediment transport was ignored.

As rain falls, the spatially varying hourly rainfall infiltrates the soil until saturation is reached. Once that occurs, ponding begins and overland flow commences. Hourly rainfall is provided by the WRF model while the infiltration rate and depth is calculated using the Green and Ampt (1911) infiltration model.

Overland flow is calculated from Manning's equation (Table 2); assuming turbulent conditions for the entire domain, while flow routing is based on the conservation of mass.

In order to satisfy the Courants-Friedrichs-Lewy (CFL) condition, the model uses a 5 second time step. All initial and boundary conditions are set to zero.

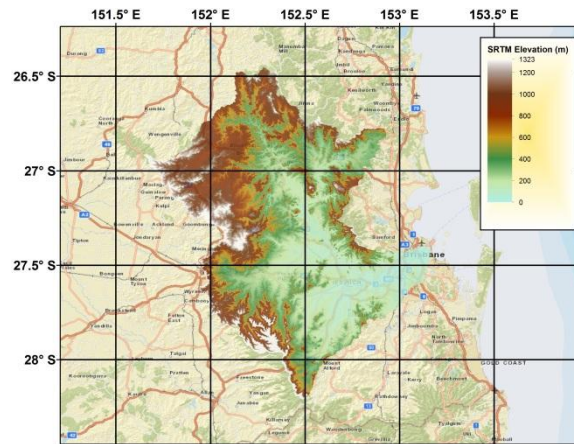


Figure 7. SRTM 90-m elevation for Brisbane River watershed.

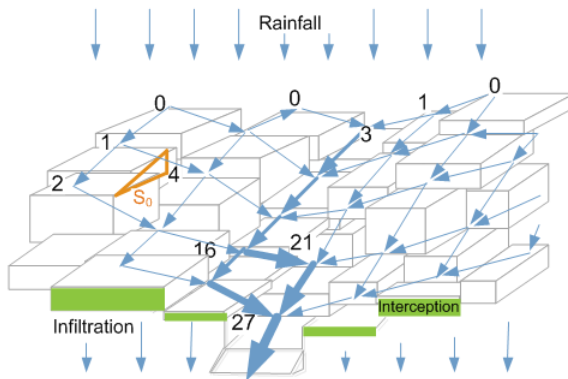


Figure 8. Conceptual diagram of the CASC2D model system.

Vegetation	Manning's n
Forests	0.075-0.30
Woodlands	0.075-0.225
Shrublands	0.075-0.12
Heathlands	0.225
Grasslands	0.075-0.12
Mangroves	0.05
Water	0.03
Cleared/Urban	0.05
Naturally bare	0.05
Regrowth	0.075

Table 2. Manning's Roughness Coefficient ( $\frac{s}{m^{1/3}}$ ) ranges used for various vegetation categories.

## 4. RESULTS

### 4.1 WRF

As discussed in section 2, the synoptic environment at the time of Wanda was dominated by a large thermal low over central Australia and a large blocking high pressure over the Tasman Sea. WRF accurately resolves these features as well as the abundant moisture across northeast Queensland (Fig. 9).

High resolution is necessary in order to resolve the mesoscale features associated with a tropical cyclone. 4-km was chosen as a compromise between computer time and resolution. Given the coarse reanalysis data and that Wanda was a relatively weak event, WRF does well in modeling the intensity (observed landfall central pressure was 994 hPa, WRF was 1004 hPa). The track error is minimal (less than 50 km) but the timing is off by 12 hours. The moist, convergent easterly flow is correctly modeled across Eastern Australia (Fig. 10).

As Wanda made landfall, the WRF modeled precipitation is highly scattered, not co-located with the center, and likely convective in nature (not shown). There is no radar data for validation. WRF reasonably models the oscillatory waves of precipitation from January 25 through January 27, 1974 (Fig 11). More importantly, post-Wanda, WRF resolves the monsoon trough that moves in on January 25 and lifts north on January 26-27. During this time, the majority of precipitation occurs along this region of convergence.

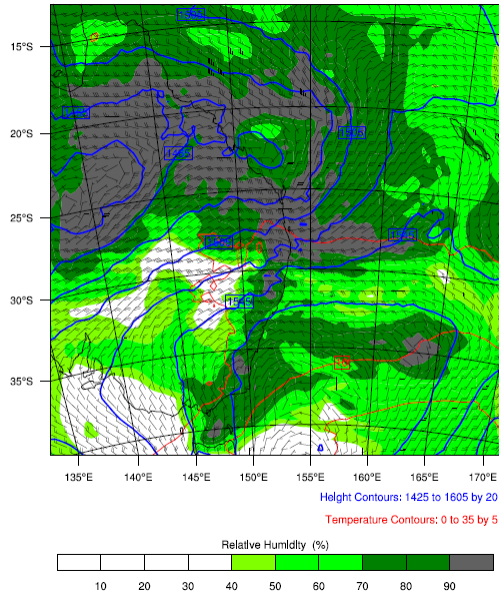


Figure 9. WRF RH (%; colors), temperature (red lines), height (blue lines), and wind velocity (kts; barbs) at the 850 hPa pressure level for January 24, 1974 00 UTC for Domain 01.

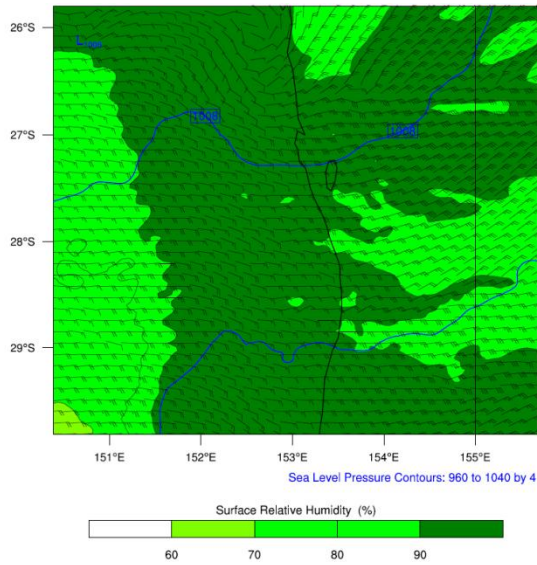


Figure 10. WRF surface RH (%; colors), wind velocity (kts; barbs), and sea level pressure (blue lines) output for January 24, 1974 20 UTC for Domain 03.

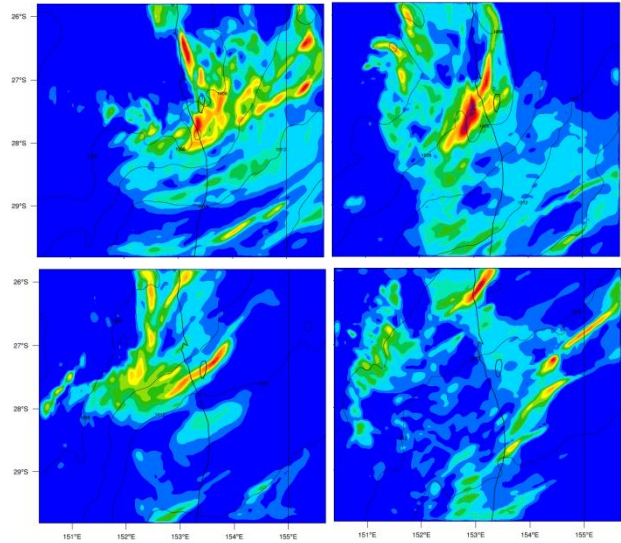


Figure 11. WRF hourly precipitation snapshots for January 25, 1974 12 UTC (top left), January 26, 1974 00 (top right) and 12 UTC (bottom left), and January 27, 1974 00 UTC (bottom right).

As a result, WRF total precipitation validates well against observations (Figs. 12 and 13) spatially (Fig. 12), as well as temporally (Fig. 14). Given all of the model uncertainties, the validation is impressive. It's important to note that orographic precipitation may be underestimated due to the resolution (Fig. 13 outlier).

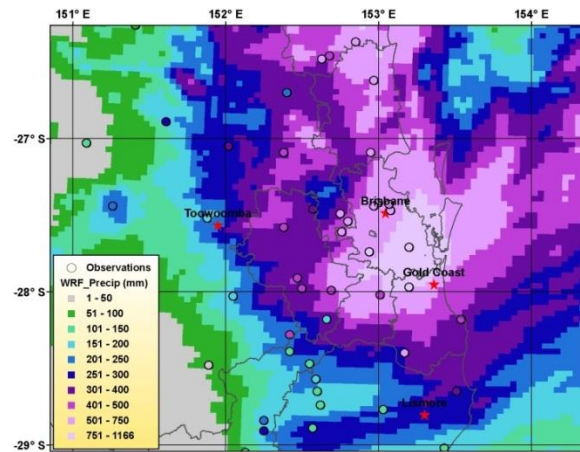


Figure 12. WRF precipitation (domain 03) as compared against observational data (circles) between January 23 and January 28, 1974.

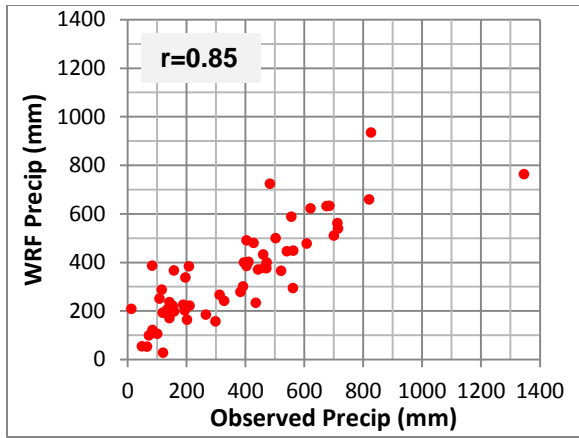


Figure 13. Scatterplot of co-located data from Figure 12.

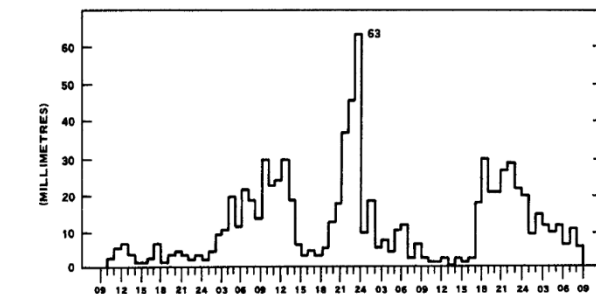
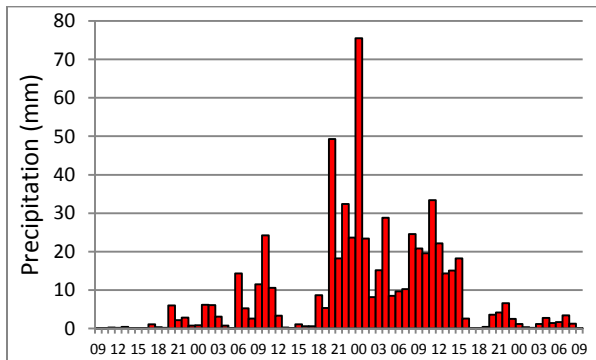


Figure 14. WRF hourly precipitation (top) versus observed (bottom) for Kedron Brook (Brisbane).

#### 4.2 CASC2D

The modified CASC2D rainfall-runoff model was then run, at 180-m resolution, using WRF-generated hourly precipitation as input. The hourly precipitation was interpolated onto the CASC2D grid using the nearest neighbor technique (all 180-m cells within a 4-km or 10-km WRF cell were assigned the same value).

The Brisbane River flooded, on average, several hundred meters off-river with some locations more than several kilometers. A comparison of maximum flood inundation between CASC2D and observations is shown in figures 15 and 16. The validation is quite good, when considering the relatively “coarse” 180-m resolution.

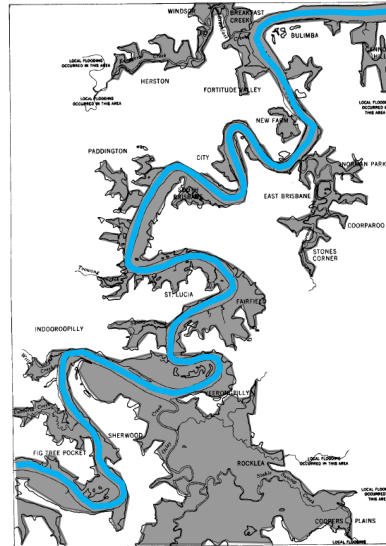


Figure 15. Observed flood inundation (Source: [http://www.bom.gov.au/hydro/flood/qld/fld\\_reports/brisbane\\_jan1974.pdf](http://www.bom.gov.au/hydro/flood/qld/fld_reports/brisbane_jan1974.pdf)).

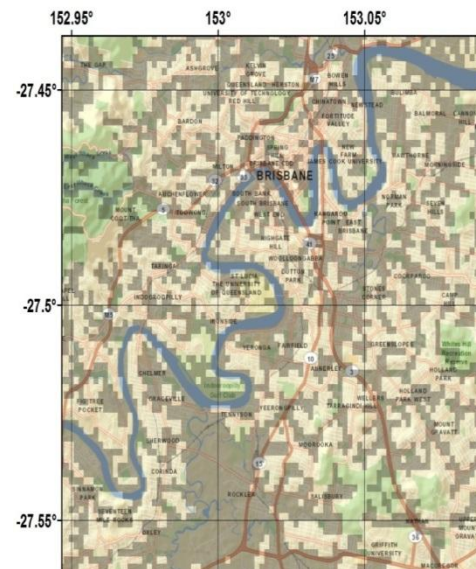


Figure 16. CASC2D flood inundation (dark brown)

Observed maximum flood depths along the Brisbane River, particularly west of town, were as high as 20-25 m with most locations between 5-15 m. Because the river is less than 100 meters wide (sub-grid) in most of these regions, it is not expected that our CASC2D simulation would resolve such magnitudes. Figure 17 compares CASC2D maximum flood depths to the few river gauge observations in the region while Figure 18 shows the flooding detail that the model is able to resolve.

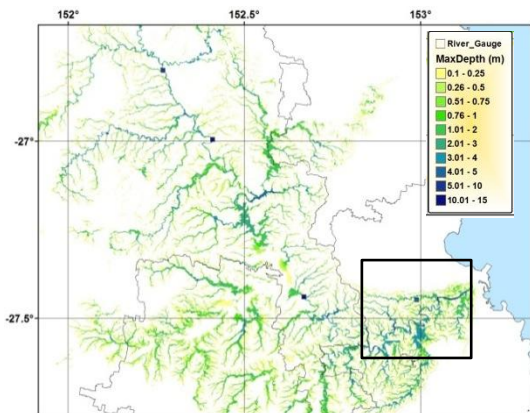


Figure 17. CASC2D maximum flood depth (m) versus river gauge observations (squares)

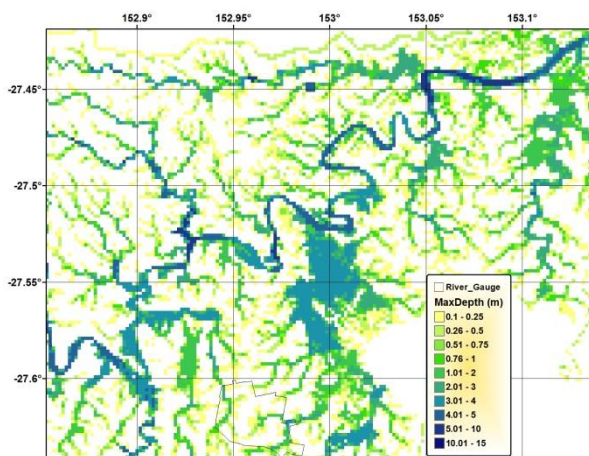


Figure 18. CASC2D maximum flood depth (m) for Brisbane region zoom-in (box inset from Figure 17).

## 5. DISCUSSION

AIR is the scientific leader and most respected provider of risk modeling software and consulting services. AIR founded the catastrophe modeling industry in 1987 and today models the risk from natural catastrophes in more than 50 countries. Using AIR's newly developed Australia Cyclone model (ACM), flood losses were calculated using the 180-m flood output from CASC2D.

For computational efficiency, ACM has a 1-km resolution within 40 km of the coast and 5-km elsewhere. The average 180-m flood depths within each 1-km and 5-km grid cells were used. Figure 19 compares flood losses from running CASC2D at 180-m and 1-km resolution. It is important to note that, again for computational efficiency, ACM has a parametric precipitation model (Fig. 20) with flood losses compared to the WRF precip run through CASC2D at 180-m. The flood losses are very similar as WRF more accurately resolves the temporal evolution of precipitation and higher resolution typically results in a smaller flood footprint (off-river) and higher flood depths.

It is also interesting to compare Wanda's loss ratio (total loss divided by total replacement value) to that of Hurricane Andrew and Cyclone Tracy (Fig.21). Even though it is substantially lower, 0.74% is quite high when considering that flood losses are typically near rivers. It provides the perspective that while Wanda was a devastating flood event and caused billions in loss to an urban area, it still doesn't quite compare to some of the more extreme wind events worldwide.

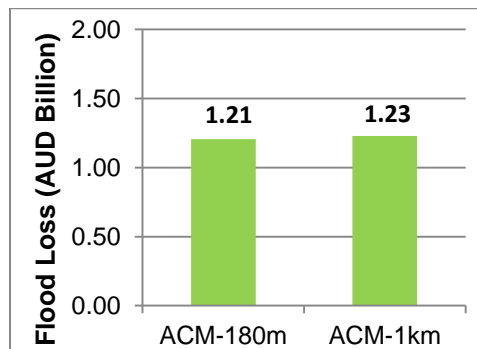


Figure 19. Flood loss comparison (Brisbane River watershed only) between ACM run at 180-m using WRF precipitation and at 1-km using AIR's parametric precipitation model.

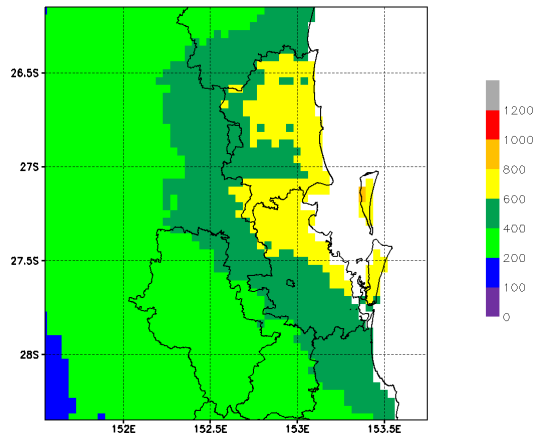


Figure 20. AIR modeled total precipitation (mm) for cyclone Wanda.

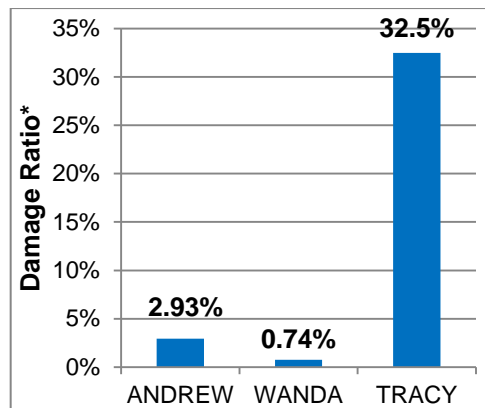


Figure 21. Loss Ratio (total loss divided by total replacement value) for Hurricane Andrew (1992), Wanda (1974), and Cyclone Tracy (1974). Total replacement value for Wanda was calculated for CASC2D flood depths exceeding 250 mm.

## 6. CONCLUSIONS

Tropical cyclone landfall intensity and damage are typically highly correlated, and yet a weak tropical cyclone caused one of the largest losses ever in Australia. A modeling case study was undertaken that coupled WRF (one-way) to a 2-D rainfall runoff model (CASC2D) and then run for cyclone Wanda (1974). Hourly precipitation from WRF was used, as input, to CASC2D. The WRF precipitation validated quite well against observational data, both in magnitude, spatial correlation, and temporal evolution. The output from CASC2D was maximum flood depths which were aggregated to the resolution of AIR's ACM. Flood losses were then calculated.

It was demonstrated that flood losses are comparable between using AIR's parametric precipitation model coupled to CASC2D at 1-km resolution and using WRF hourly precipitation coupled to CASC2D at 180-m resolution. It was also demonstrated that no matter which approach or resolution is used, CASC2D flood magnitudes are too low likely because the rivers tend to be sub-grid and because channel flow is ignored. To prove this point, CASC2D was run at 90-m using AIR's parametric precipitation model and the average magnitude difference, in the rivers, between 90-m and 1-km simulations was several factors (not shown).

Realistically, CASC2D should be run at no less than 30-m resolution with channel flow turned on to very accurately resolve riverine processes. However, from an aggregate perspective, coarser resolution overland flow is a reasonable compromise between accuracy and computational efficiency (AIR tropical cyclone models provide at least 10,000 years of simulated risk) and still result in realistic estimates of flood damage.

## 7. REFERENCES

- Australia Bureau of Meteorology best track data:  
<http://www.bom.gov.au/cyclone/history/index.shtml>
- Australia Population Density:  
<http://www.abs.gov.au/AUSSTATS/abs@.nsf/Lookup/4613.0Chapter20Jan+2010>
- Brisbane Floods January 1974:  
[http://www.bom.gov.au/hydro/flood/qld/fld\\_reports/brisbane\\_jan1974.pdf](http://www.bom.gov.au/hydro/flood/qld/fld_reports/brisbane_jan1974.pdf)
- Courant R., K. Friedrichs, and H. Lewy, 1967: On the partial difference equations of mathematical physics, *IBM Journal*, 215–234.
- Farr, T. G., et al., 2007: The Shuttle Radar Topography Mission. *Reviews of Geophysics*, 45(2), 1-33.
- McKenzie N.J., D.W. Jacquier, L.J. Ashton, and H.P. Cresswell, 2000: Estimation of Soil Properties using the Atlas of Australian Soils. CSIRO Land and Water Technical Report 11/00.
- Rayner, D.P. 2005: Australian Synthetic Daily Class A Pan Evaporation. Queensland Department of Natural Resources and Mines. Australian Government Department of the Environment and Water Resources.

Rojas, R., P. Julien, and B. Johnson, 2003: A 2-Dimensional Rainfall-Runoff and Sediment Model. Colorado State University.

Skamarock, W. C., J. B. Klemp, J. Dudhia, D. O. Gill, D. M. Barker, W. Wang, and J. G. Powers, 2005: A description of the Advanced Research WRF Version 2. NCAR Tech Notes-468+STR.